A&A 534, A95 (2011)
DOI: 10.1051/0004-6361/201117154

Astronomy & Astrophysics

Calibrating the Cepheid period-luminosity relation from the infrared surface brightness technique

II. The effect of metallicity and the distance to the LMC⋆,⋆⋆

J. Storm[1], W. Gieren[2], P. Fouqué[3], T. G. Barnes[4], I. Soszyński[5], G. Pietrzyński[2,5], N. Nardetto[2,6], and D. Queloz[7]

[1] Leibniz-Institut für Astrophysik Potsdam (AIP), An der Sternwarte 16, 14482 Potsdam, Germany
e-mail: jstorm@aip.de
[2] Universidad de Concepción, Departamento Astronomía, Casilla 160-C, Concepción, Chile
[3] IRAP, Université de Toulouse, CNRS, 14 Av. E. Belin, 31400 Toulouse, France
[4] University of Texas at Austin, McDonald Observatory, 82 Mt. Locke Rd, McDonald Observatory, TX 79734, USA
[5] Warsaw University Observatory, Al. Ujazdowskie 4, 00-478 Warsaw, Poland
[6] Laboratoire Fizeau, UNS/OCA/CNRS UMR6525, Parc Valrose, 06108 Nice Cedex 2, France
[7] Observatoire Astronomique de l'Université de Genève, Chemin de Maillettes 51, 1290 Sauverny, Switzerland

Received 28 April 2011 / Accepted 23 July 2011

ABSTRACT

Context. The extragalactic distance scale builds directly on the Cepheid period-luminosity (PL) relation as delineated by the sample of Cepheids in the Large Magellanic Cloud (LMC). However, the LMC is a dwarf irregular galaxy, quite different from the massive spiral galaxies used for calibrating the extragalactic distance scale. Recent investigations suggest that not only the zero-point but also the slope of the Milky Way PL relation differ significantly from that of the LMC, casting doubts on the universality of the Cepheid PL relation.

Aims. We want to make a differential comparison of the PL relations in the two galaxies by delineating the PL relations using the same method, the infrared surface brightness method (IRSB), and the same precepts. We furthermore extend the metallicity baseline for investigating the zero-point dependence, by applying the method to five SMC Cepheids as well.

Methods. The IRSB method is a Baade-Wesselink type method to determine individual distances to Cepheids. We apply a newly revised calibration of the method as described in an accompanying paper (Paper I) to 36 LMC and five SMC Cepheids and delineate new PL relations in the $V, I, J, \& K$ bands as well as in the Wesenheit indices in the optical and near-IR.

Results. We present 509 new and accurate radial velocity measurements for a sample of 22 LMC Cepheids, enlarging our earlier sample of 14 stars to include 36 LMC Cepheids. The new calibration of the IRSB method is directly tied to the recent HST parallax measurements to ten Milky Way Cepheids, and we find a LMC barycenter distance modulus of 18.45 ± 0.04 (random error only) from the 36 individual LMC Cepheid distances. In the J, K bands we find identical slopes for the LMC and Milky Way PL relations and only a weak letallicity effect on the zero points (consistent with a zero effect), metal poor stars being fainter. In the optical we find the Milky Way slopes are slightly shallower than the LMC slopes (but again consistent with no difference in the slopes) and small effects on the zero points. However, the important Wesenheit index in V, $(V - I)$ shows a metallicity effect on the slope and on the zero point which is likely to be significant.

Conclusions. We find a significant metallicity effect on the W_{VI} index $\gamma(W_{VI}) = -0.23 \pm 0.10$ mag dex^{-1} as well as an effect on the slope. The K-band PL relation on the other hand is found to be an excellent extragalactic standard candle being metallicity insensitive in both slope and zero-point and at the same time being reddening insensitive and showing the least internal dispersion.

Key words. stars: variables: Cepheids – stars: fundamental parameters – stars: distances – Magellanic Clouds – distance scale

1. Introduction

The Cepheid period-luminosity (PL-) Relation is fundamental to the calibration of the extra-galactic distance scale and thus to the determination of the Hubble constant. Modern reviews on the calibration of the Cepheid distance scale can be found in e.g. Freedman & Madore (1991), Fouqué et al. (2003), Sandage & Tammann (2006), Fouqué et al. (2007), and Barnes (2009) while Freedman & Madore (2010) review the present status of the quest for the Hubble constant. A dissenting view can be found e.g. in Sandage et al. (2009) and references therein.

The value of the PL relation rests with its universality, in particular that the PL relation slope and zero points are independent of metallicity. The zero point has long been suggested to be metallicity dependent and the HST key project on the extragalactic distance scale (Freedman et al. 2001) corrected for this based on the empirical studies available at that time (e.g. Freedman & Madore 1990; Sasselov et al. 1997; Kochanek 1997; Kennicutt et al. 1998) with an estimated effect in the W_{VI} index of -0.2 ± 0.2 mag dex^{-1} in the sense that metal-poor Cepheids are fainter than metal-rich Cepheids. However, the size and even the sign of the effect is still disputed.

⋆ Based on observations collected at the European Organisation for Astronomical Research in the Southern Hemisphere, Chile, Programme-IDs 076-C.0158, 078.D-0299, & 080.D-0318.

⋆⋆ Full Table 2 is only available at the CDS via anonymous ftp to cdsarc.u-strasbg.fr (130.79.128.5) or via http://cdsarc.u-strasbg.fr/viz-bin/qcat?J/A+A/534/A95

Udalski et al. (2001) found no effect on the slope nor on the zero-point when comparing the metal-poor Cepheids of IC 1613 with those in the Magellanic Clouds based on TRGB distances to those galaxies. On the other hand Romaniello et al. (2008) found a significant effect with the opposite sign when comparing Milky Way and Magellanic Cloud Cepheids with individual spectroscopic metallicity determinations. Sakai et al. (2004) and Storm et al. (2004), found an effect of similar size and sign as that adopted by the HST key project, but the latter study also showed a significant difference in the slopes of the Milky Way and LMC relations, as also found by Sandage et al. (2004). Recently Bono et al. (2010) have argued for no significant effect in the W_{VI} and W_{JK} index on the basis of empirical as well as theoretical arguments.

Observationally, we are in the dilemma of either using a large sample of Cepheids, like in the Large Magellanic Cloud (LMC), which constrains very well the slope of the relation for a low metallicity sample of stars and which leaves the zero point to be determined from secondary indicators, or of using direct geometric distances (parallaxes) to a handful of nearby, solar metallicity, Milky Way Cepheids which constrain well the zero point of the PL relation but which do not constrain the slope very well.

Baade-Wesselink type methods which use the pulsational properties of the Cepheids to determine direct distances to individual Cepheids promise to resolve this dilemma by yielding direct individual distances to a large sample of Milky Way and Magellanic Cloud Cepheids spanning a significant range of metallicities. In particular, the near-infrared surface brightness (IRSB) method (Fouqué & Gieren 1997), a near-infrared variant of the Barnes-Evans method (Barnes & Evans 1976) shows great promise in achieving this goal as it is insensitive to reddening errors. The technique has also been shown to be independent of the metallicity of the Cepheids (Storm et al. 2004). A few years ago the IRSB method was re-calibrated using interferometrically measured, phase-resolved angular diameters of Cepheids by Kervella et al. (2004). This was an extremely important achievement as it proved that the pulsating Cepheid variables indeed obey the same surface brightness-colour relation as the stable yellow giant stars which were used to construct the surface brightness-colour relation adopted in the original calibration of the technique (Fouqué & Gieren 1997). The improved version of the IRSB technique was then applied to Milky Way Cepheids by Storm et al. (2004) and Groenewegen (2008), and for the first time to extragalactic Cepheids by Storm et al. (2004) (SMC) and Gieren et al. (2005a) (LMC).

In our earlier application of the method to Milky Way Cepheids (Storm et al. 2004), we found that the slopes of the resulting PL relations in all optical and near-infrared bands were significantly steeper than the those directly observed in the Large Magellanic Cloud by the OGLE Project and by Persson et al. (2004), thus challenging the universality of the PL relation. Gieren et al. (2005a) then analyzed thirteen LMC Cepheids, for which the data required for the IRSB analysis were available at the time, in an identical fashion and found that the PL relation slopes in the LMC were very similar to the one obtained for the Milky Way sample, but different from the observed apparent slope of the LMC sample. We interpreted this as evidence for the existence of an as yet undetected period-dependent systematic error in the IRSB method, but the limited size of the LMC sample prevented firm conclusions.

To put our previous analysis on a firmer basis, we present in the present paper new and very accurate radial velocity curves for 22 additional LMC Cepheids (Sect. 2) thus almost tripling the existing sample for an IRSB analysis to a total of 36 stars.

Table 1. LMC Cepheids for which we have obtained new radial velocity curves with the HARPS and FEROS high-resolution spectrographs at ESO-La Silla.

HV873	HV914	HV2405	HV12452
HV876	HV1005	HV2527	HV12505
HV877	HV1006	HV2538	HV12717
HV878	HV1023	HV2549	U1
HV881	HV2282	HV5655	
HV900	HV2369	HV6093	

To allow a purely differential comparison with solar metallicity Cepheids we present a similar analysis for 77 Milky Way Cepheids in an accompanying paper (Storm et al. 2011, hereinafter Paper I). In that paper we also combine the new empirical constraints on the projection (p-)factor, converting Cepheid radial into pulsational velocities, as obtained from the present LMC study and the recent HST parallax measurements to ten Galactic Cepheids (Benedict et al. 2007), to obtain a new empirical calibration of the p-factor relation to be used in our IRSB distance analysis.

In Sect. 3 We briefly describe the IRSB method in its present form and we discuss the choice of the p-factor relation. We present the resulting LMC period-luminosity relations in optical and near-infrared bands in Sect. 4 where we also compare to the SMC and Milky Way samples to estimate the effect of metallicity on the PL relations. In Sect. 5 we discuss our results and compare them to other recent investigations. Section 6 summarizes our results.

2. The data

2.1. The LMC Cepheid sample

We have selected 22 Cepheids in the LMC (see Table 1) showing a wide range of periods, all having high-quality near-IR lightcurves from Persson et al. (2004) and very accurate optical photometry from OGLE-III (Udalski et al. 2008; Soszyński et al. 2008). From their optical lightcurves, all these Cepheids are clearly fundamental mode pulsators. For these stars we have obtained radial velocity curves as will be described in the next section. A typical data set (HV 2282) is shown in Fig. 1.

Gieren et al. (2005a) performed a first IRSB analysis on a sample of 13 Cepheids in the LMC, six of which belonging to the young blue, massive cluster NGC 1866. These stars will all be used in the following analysis. To this sample we have added the star HV2827. The radial velocity data for this star comes from Imbert et al. (1987), the optical photometry from Moffet et al. (1998) and the near-IR photometry from Persson et al. (2004). For all the stars we have transformed the near-IR photometry to the SAAO system using first the transformations given by Persson et al. (2004) to transform the LCO data to the CTIO system, and then applying the transformations given by Carter (1990) to transform from the CTIO to the SAAO system. In this way we ensure to be on a common system with the Milky Way sample presented in the accompanying Paper I, and to be on the same photometric system which was used by Kervella et al. (2004) for the calibration of the surface-brightness versus colour relation.

2.2. Spectroscopic data

Using the HARPS instrument on the ESO 3.6 m telescope and the FEROS instrument on the ESO/MPG 2.2 m telescope, both

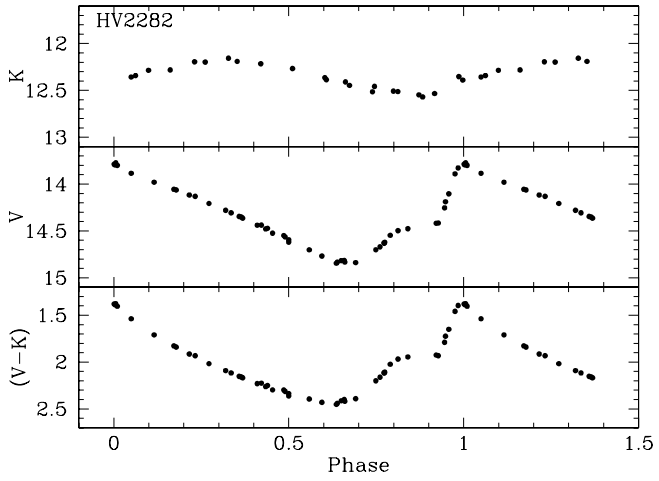

Fig. 1. The photometric V and K light curves, and the $(V-K)$ colour curve as used in our IRSB analysis for the LMC Cepheid variable HV2282. This is a typical set of photometric light and colour curves in the present study based on the optical photometry from OGLE-III (Udalski et al. 2008; Soszyński et al. 2008), and the near-IR photometry from Persson et al. (2004).

at ESO La Silla, Chile, we have obtained 509 new radial velocity measurements for the above described sample of 22 LMC Cepheids. HARPS was used for 20 of the stars while FEROS was used for two additional Cepheids, HV914 and HV12717.

HARPS (Mayor et al. 2003) is a fiber-fed cross-dispersed echelle spectrograph mounted inside a vacuum vessel for improved wavelength stability. It has a spectral resolution of R = 115 000 (3.2 pix) and the wavelength range reaches from 380 to 690 nm. HARPS was used to observe 20 LMC Cepheids in the sample. Radial velocity observations were obtained during a single, 16-night, visitor observing run in December 2005 which were later complemented with service mode observations in the following two seasons to cover phase gaps in the velocity curves.

We used the standard reduction pipeline using cross-correlation with a G2-type spectral mask (Baranne et al. 1996; Pepe et al. 2002) to extract radial velocities from the spectral data.

FEROS (Kaufer et al. 1999) is also a fiber-fed crossed-dispersed spectrograph. It has a resolution of R = 48 000 (2.2 pix) covering the wavelength range from 360 to 920 nm. The Cepheid radial velocities were extracted using the cross-correlation method with the FEROS pipeline.

Both instruments are known to be very stable with wavelength drifts well below 100 m/s. As our main objective was to obtain well covered, accurate radial velocity curves we made relatively short exposures with resulting low signal to noise ratios of 5 to 10. This was found sufficient to keep the errors of the individual radial velocity measurements below 100 m/s, which meets the precision we desired.

The Heliocentric Julian dates and the individual radial velocities are tabulated in Table 2 and the radial velocity curves are plotted in Fig. 2. A few data points appear to be misidentifications as they are close to the systemic velocity of the star but do not fall on the velocity curve (see HV873, HV878, and U1). They have been marked with crosses in the figure and are not considered in the further analysis. In the case of HV1005 we found two points with similar offsets from the radial velocity curve. These two data points were obtained two years later than the majority of the data, obtained during the sixteen consecutive nights (see above), thus suggesting the possibility of orbital motion for this star. We have simply disregarded those two points in the following analysis.

Table 2. New radial velocities for the 22 LMC Cepheids.

ID	HJD (days)	RV (km s^{-1})
HV873	2 453 701.7205	247.46
HV873	2 453 702.7489	250.14
HV873	2 453 703.7567	252.64
HV873	2 453 704.7536	255.15
HV873	2 453 705.7469	257.52
HV873	2 453 706.7521	259.96
...	...	...

Notes. The complete table is available in the electronic form from the CDS.

3. The IRSB method

3.1. The surface brightness-colour relation

The infrared surface brightness (IRSB) method is a variant of the Baade-Wesselink method originally developed by Barnes & Evans (1976) in the optical spectral range. It matches the angular diameter variation of a Cepheid as determined from photometry, with the radius variation of the pulsating star as determined from an integration of its pulsational velocity curve.

In Paper I we present a more detailed discussion of the method, which relates the surface brightness parameter, F_V, to a colour index $(V-K)_0$ to determine the angular diameter variation of the star.

Here we use the relation

$$F_V = 4.2207 - 0.1V_0 - 0.5\log\theta \quad (1)$$

$$= -0.1336(V-K)_0 + 3.9530 \quad (2)$$

as determined by Kervella et al. (2004).

3.2. The projection factor

Knowledge of the projection (p-) factor which converts an observed radial velocity of a Cepheid into the pulsational velocity at its surface is crucial for any kind of Baade-Wesselink analysis. The p-factor has to take into account not only the geometrical projection effects across the observed stellar disk but also fold this with the effect of limb darkening and possibly take into consideration non-LTE effects due to the dynamic behaviour of the pulsating atmosphere.

Recent empirical (Gieren et al. 2005a) and theoretical (Nardetto et al. 2007, 2009) work has shown that the p-factor relation from Hindsley & Bell (1989), which shows a slight period dependence of the p-factor and was used in our early work (Gieren et al. 1993), is not appropriate. In fact the new data presented here (see Sect. 4.3) largely supports the empirical findings of Gieren et al. (2005a) that the p-factor depends quite strongly on pulsational period or the derived distances to the LMC Cepheids become period dependent, which is clearly unphysical. We have discussed this issue in more detail in Paper I. In that paper, we find the best fitting relation to be:

$$p = 1.550(\pm0.04) - 0.186(\pm0.06)\log P \quad (3)$$

which we will adopt here.

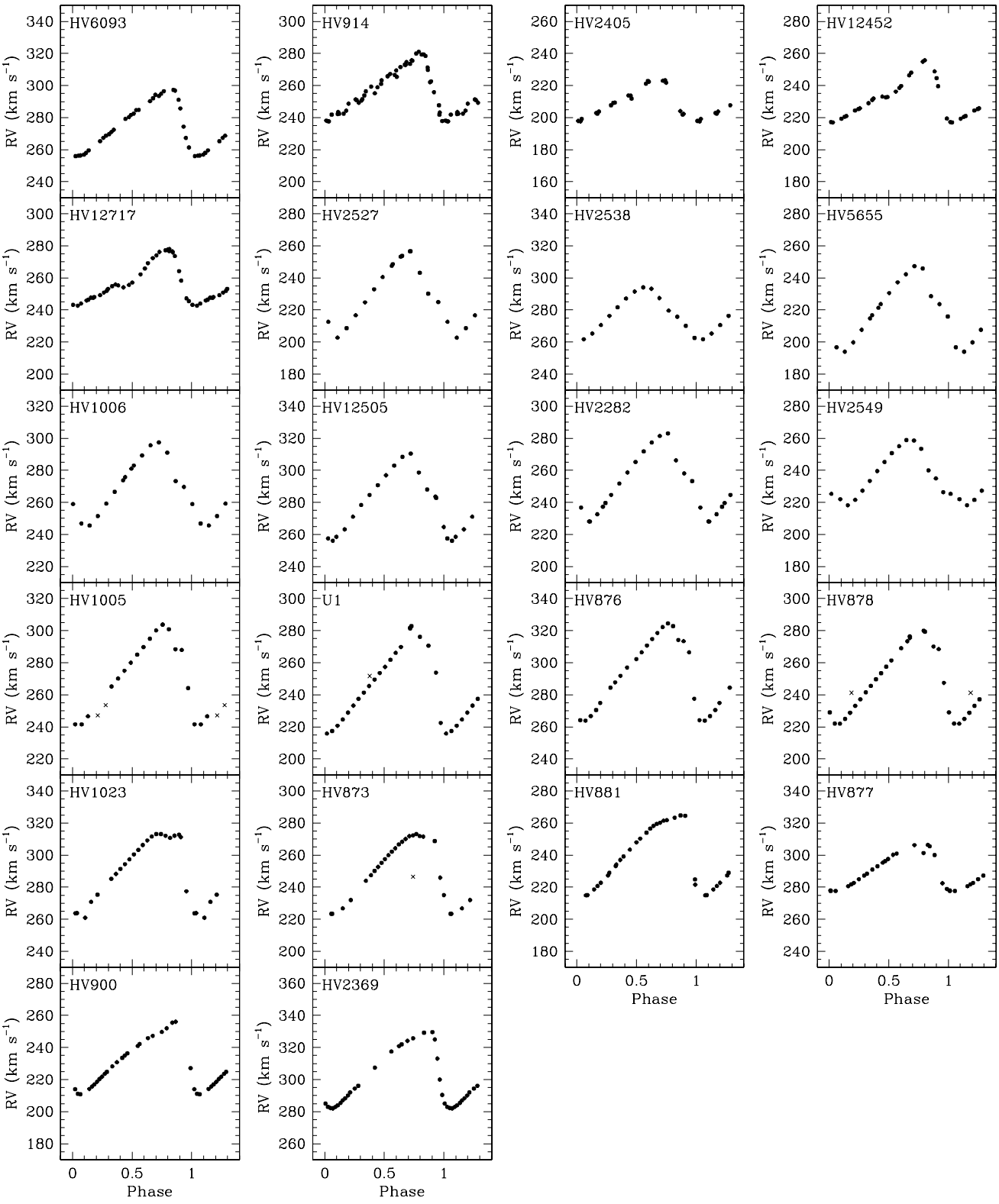

Fig. 2. The new radial velocity curves for 22 LMC Cepheids from HARPS and FEROS (HV 914 and HV 12717) data. The crosses indicate points that have not been used in the analysis. The radial velocity range in each panel is 120 km s^{-1} so the amplitudes in the panels are directly comparable. The panels are arranged according to increasing pulsational period.

It is important to note that the exact choice of the *p*-factor relation has no bearing on the conclusions regarding the effect of metallicity on the PL relations in the present paper, as long as the *p*-factor relation used in the analysis is the same for both samples, the Milky Way and the LMC. Any change in the relation would affect both Milky Way and LMC Cepheids in the same way but the differentials would remain the same. This of course is based on the implicit assumption that the *p*-factor is independent of metallicity. Work is currently underway to further investigate this point.

3.3. The reddening

The reddenings for the LMC stars were taken from the catalogue of Persson et al. (2004) whenever possible. For the NGC 1866 stars we adopted values of $E(B-V) = 0.06$ following the discussion in Storm et al. (2005). The reddening is very low for all the stars and the star-to-star variation is very low as well, so reddening errors can only marginally affect the resulting period-luminosity relations, even in the optical bands. We have adopted the reddening law from Cardelli et al. (1989) with a total-to-selective absorption of $R_V = 3.23$ following the discussion in Fouqué et al. (2007). In this way we are proceeding exactly in the same way as for the Milky Way Cepheids in Paper I.

3.4. Adopted metallicity

We adopt the mean metallicity estimates for the Milky Way, LMC and SMC Cepheids from the discussion by Luck et al. (1998) based on new and literature measures for Cepheids and supergiants. They find for the Milky Way [Fe/H] = +0.03 based on 69 stars with $\sigma = 0.14$, for the LMC [Fe/H] = −0.34 based on 32 stars with $\sigma = 0.15$ and for the SMC [Fe/H] = −0.68 based on 25 stars with $\sigma = 0.13$. These values are largely supported by Romaniello et al. (2008) who found values of −0.30 dex and −0.75 dex respectively. We note that the Cepheids in NGC 1866 might be slightly more metal-poor, [Fe/H] = −0.5, based on the spectroscopic study of three cluster giants by Hill et al. (2000) and the photometric measurement for NGC 1866 of -0.48 ± 0.18 by Hilker et al. (1995) from Strömgren photometry, but we do not make this distinction in the following.

4. Results

4.1. Distances and absolute magnitudes

We have applied the IRSB method as described in the previous section to find the distances and absolute magnitudes for the LMC Cepheids reported in Table 3 and for the SMC sample of Storm et al. (2004) in Table 4. The absolute magnitudes are intensity-averaged magnitudes.

4.2. The distances to the LMC and the SMC

On the basis of the individual distances to the Cepheids in the LMC we can now determine the distance to the LMC barycenter. First we correct the measured distance of each Cepheid by the distance offset from the LMC disk model of van der Marel & Cioni (2001) as tabulated in the last column of Table 3 and then compute the mean of the resulting values. We find $(m-M)_0(LMC) = 18.45 \pm 0.04$ (random error only) with a standard deviation of 0.22 mag. As the Cepheids are well distributed across the face of the LMC the uncorrected mean modulus is identical to within 0.01 mag to the adopted barycentric distance modulus value.

For the SMC we only have five stars so the random error is significantly larger than is the case for the LMC. Additionally, the SMC is well known to exhibit more pronounced depth effects than the LMC, so some additional scatter is to be expected. We find from the five Cepheids an unweighted mean value of $(m-M)_0$(SMC) = 18.92 ± 0.14 with a standard deviation of 0.32 mag. The offset in modulus with respect to the LMC of 0.47 mag is in excellent agreement with the very accurate value of 0.44 ± 0.05 mag found by Cioni et al. (2000) from an investigation of a large sample of tip of the red-giant branch (TRGB) stars in the reddening insensitive near-infrared, thus giving us confidence that our five stars are indeed representative of the SMC as a whole.

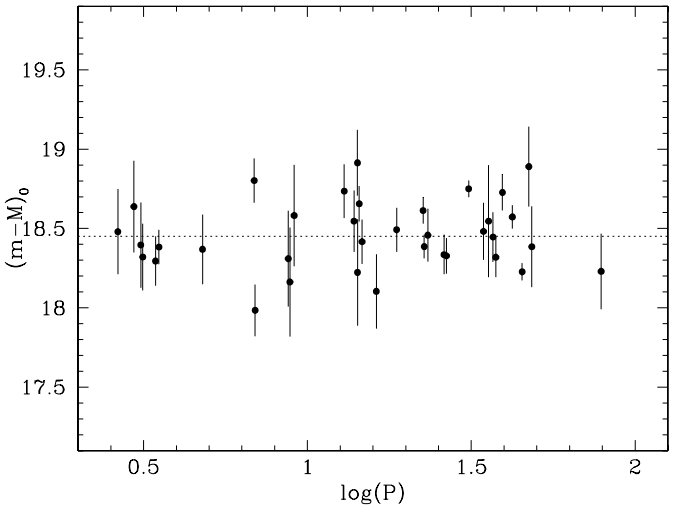

Fig. 3. The IRSB-based distance moduli of 36 Cepheids in the LMC using the new p-factor relation derived in Paper I, plotted as a function of their pulsation period. The moduli have been referred to the LMC barycenter using the LMC disk model of van der Marel & Cioni (2001).

4.3. Constraints on the p-factor relation

As discussed in Sect. 3.2 we can use the IRSB distances to the 36 LMC Cepheids to place constraints on the p-factor relation. We have rederived the distances to the individual LMC Cepheids using different p-factor relations, as discussed in more detail in Paper I, and we computed the individual LMC barycentric distances as before. In Table 5 we list the resulting mean LMC distance moduli as well as the slope of the distance modulus as a function of pulsation period, for each of the p-factor relations we tested in this process. The function distance modulus versus pulsation period must of course have a zero slope, and with the present large sample of 36 stars we are able to place strong constrains on the slope. In the table it can be seen that the original Hindsley & Bell (1989) relation gives a very plausible LMC distance but a strong and unphysical period dependence of the distance moduli. Similarly the Nardetto et al. (2009) relation gives a slope which deviates at the level of 2σ from the uncorrelated relation and the LMC distance becomes uncomfortably short at 18.26 mag. The third relation uses the slope of the p-factor relation from Nardetto et al. (2009) but with a zero point which yields IRSB distances to Milky Way Cepheids in agreement with the recent parallaxes from Benedict et al. (2007). The last column corresponds to the relation derived in Paper I which we have adopted here, which yields LMC Cepheid distance moduli which are totally independent of their pulsation period. This is borne out in Fig. 3 where we show the LMC center distance moduli based on the individual LMC Cepheid moduli corrected for the disk model of van der Marel and Cioni (2001) as a function of log P. It is evident that with the adopted p-factor relation there is no significant correlation between pulsational period and derived distance to the LMC Cepheids.

Table 3. Distances and absolute magnitudes for the LMC Cepheids calculated using the precepts given in Paper I, using the new p-factor relation.

(1) ID	(2) log(P)	(3) d (kpc)	(4) $\sigma(d)$ (kpc)	(5) $(m-M)_0$ (mag)	(6) $\sigma_{(m-M)}$ (mag)	(7) M_V (mag)	(8) M_I (mag)	(9) M_J (mag)	(10) M_H (mag)	(11) M_K (mag)	(12) W_{VI} (mag)	(13) W_{JK} (mag)	(14) $E(B-V)$ (mag)	(15) $\Delta\phi$	(16) $\Delta(m-M)$ (mag)
HV 12199	0.421469	49.7	1.8	18.48	0.08	−2.41	−3.01	−3.13		−3.80	−3.94	−4.26	0.060	0.035	−0.058
HV 12203	0.470427	53.4	2.1	18.64	0.09	−2.71	−3.31	−3.66		−4.08	−4.24	−4.37	0.060	0.050	−0.058
HV 12202	0.491519	47.8	1.7	18.40	0.08	−2.53	−3.14	−3.60		−4.02	−4.09	−4.30	0.060	0.030	−0.058
HV 12197	0.497456	46.1	1.3	18.32	0.06	−2.42	−3.07	−3.44		−3.87	−4.07	−4.17	0.060	−0.015	−0.057
HV 12204	0.536402	45.6	1.0	18.30	0.05	−2.79	−3.33	−3.67		−4.07	−4.17	−4.34	0.060	0.015	−0.059
HV 12198	0.546887	47.5	0.7	18.38	0.03	−2.63	−3.27	−3.69		−4.09	−4.26	−4.36	0.060	0.020	−0.059
HV 6093	0.679885	47.2	1.4	18.37	0.06	−3.25	−3.86	−4.21		−4.60	−4.79	−4.87	0.058	−0.015	−0.048
HV 914	0.837489	57.6	1.1	18.80	0.04	−4.10	−4.79	−5.18	−5.54	−5.59	−5.84	−5.88	0.070	−0.035	0.013
HV 2405	0.840331	39.5	0.9	17.98	0.05	−3.06	−3.77	−4.14	−4.52	−4.57	−4.86	−4.86	0.070	−0.015	0.046
HV 12452	0.941457	45.9	1.9	18.31	0.09	−3.74	−4.48	−4.94	−5.32	−5.37	−5.62	−5.67	0.058	0.030	0.058
HV 12717	0.946628	42.9	2.0	18.16	0.10	−3.62	−4.33	−4.77	−5.14	−5.21	−5.42	−5.51	0.058	−0.005	0.065
HV 12816	0.959466	52.0	2.3	18.58	0.09	−4.29	−4.88	−5.24	−5.56	−5.62	−5.79	−5.88	0.070	0.015	−0.075
HV 2527	1.112251	55.8	1.3	18.73	0.05	−4.36	−5.21	−5.66	−6.09	−6.15	−6.51	−6.49	0.070	0.005	0.041
HV 2538	1.142118	51.2	1.3	18.55	0.06	−4.39	−5.28	−5.70	−6.14	−6.19	−6.64	−6.53	0.100	−0.040	−0.019
HV 5655	1.152657	60.7	1.7	18.91	0.06	−4.69	−5.53	−5.96	−6.41	−6.47	−6.84	−6.81	0.100	−0.015	0.046
HV 1006	1.152786	44.1	2.0	18.22	0.10	−4.17	−4.95	−5.48	−5.90	−5.95	−6.15	−6.28	0.100	0.005	−0.010
HV 12505	1.158115	53.9	0.8	18.66	0.03	−4.14	−5.04	−5.63	−6.11	−6.17	−6.43	−6.55	0.100	−0.005	0.031
HV 2282	1.166636	48.2	0.9	18.42	0.04	−4.41	−5.19	−5.66	−6.07	−6.12	−6.38	−6.44	0.100	0.015	0.051
HV 2549	1.210289	41.8	1.3	18.10	0.07	−4.50	−5.31	−5.69	−6.06	−6.13	−6.56	−6.43	0.058	0.020	0.052
HV 1005	1.272209	49.9	0.9	18.49	0.04	−4.72	−5.47	−5.98	−6.41	−6.45	−6.62	−6.77	0.100	0.015	−0.023
U1	1.353098	52.8	0.6	18.61	0.02	−4.82	−5.70	−6.28	−6.74	−6.80	−7.07	−7.16	0.100	0.010	0.060
HV 876	1.356342	47.6	0.5	18.39	0.02	−5.06	−5.86	−6.27	−6.67	−6.71	−7.10	−7.02	0.100	0.005	0.005
HV 878	1.367445	49.2	1.1	18.46	0.05	−5.11	−5.66	−6.35	−6.75	−6.80	−6.52	−7.12	0.058	−0.010	0.055
HV 12815	1.416910	46.5	0.8	18.34	0.04	−5.08	−5.96	−6.48	−6.94	−6.99	−7.32	−7.35	0.070	−0.030	−0.075
HV 1023	1.424235	46.3	0.7	18.33	0.03	−4.77		−6.28	−6.75	−6.79		−7.15	0.070	0.025	−0.049
HV 899	1.492039	56.2	0.4	18.75	0.01	−5.71	−6.52	−7.02	−7.45	−7.50	−7.78	−7.82	0.110	0.025	0.018
HV 873	1.537311	49.7	1.2	18.48	0.05	−5.87		−7.08	−7.46	−7.50		−7.79	0.130	−0.010	0.080
HV 881	1.552820	51.2	2.5	18.55	0.10	−5.55		−6.97	−7.41	−7.50		−7.85	0.030	−0.065	0.062
HV 879	1.566167	48.9	1.0	18.45	0.05	−5.27	−6.25	−6.84	−7.32	−7.39	−7.75	−7.78	0.060	0.015	0.044
HV 909	1.574986	46.1	0.8	18.32	0.04	−5.75	−6.52	−6.97	−7.36	−7.43	−7.70	−7.74	0.058	−0.065	0.048
HV 2257	1.595153	55.6	0.8	18.73	0.03	−5.90	−6.80	−7.35	−7.81	−7.87	−8.19	−8.22	0.060	−0.005	0.054
HV 2338	1.625350	51.8	0.5	18.57	0.02	−5.95	−6.83	−7.36	−7.80	−7.86	−8.19	−8.21	0.040	−0.015	0.070
HV 877	1.655215	44.2	0.3	18.23	0.02	−5.21		−6.80	−7.31	−7.36		−7.74	0.100	0.070	0.017
HV 900	1.675637	60.0	2.0	18.89	0.07	−6.32		−7.72	−8.17	−8.25		−8.62	0.058	−0.060	0.042
HV 2369	1.684646	47.5	1.6	18.39	0.07	−6.02		−7.46	−7.90	−7.96		−8.29	0.095	0.005	−0.029
HV 2827	1.896354	44.3	1.4	18.23	0.07	−6.18	−7.20	−7.81	−8.29	−8.36	−8.75	−8.73	0.080	0.035	−0.079

Notes. In Cols. 3 and 4 we give the IRSB distance and the associated error estimate. In Cols. 5 and 6 follows the distance modulus, and in Cols. 7 through 13, we give the absolute magnitudes in the different bands as well as the Wesenheits indices. Finally in Col. 14 we give the adopted reddening and in Col. 15 the adopted phase shift between spectroscopic and photometric angular diameters. Column 16 gives the magnitude correction to refer the distance moduli to the LMC barycenter.

Table 4. Distances and absolute magnitudes for the SMC Cepheids calculated by using the same precepts as in Table 3.

ID	log P	d (kpc)	$\sigma(d)$ (kpc)	$(m-M)_0$ (mag)	$\sigma_{(m-M)}$ (mag)	M_V (mag)	M_I (mag)	M_J (mag)	M_K (mag)	W_{VI} (mag)	W_{JK} (mag)	$E(B-V)$ (mag)	$\Delta\phi$
HV 1345	1.129638	55.5	1.8	18.72	0.07	−4.06	−4.80	−5.41	−5.88	−5.96	−6.20	0.030	0.025
HV 1335	1.157807	59.9	1.6	18.89	0.06	−4.37	−5.06	−5.56	−5.95	−6.12	−6.21	0.090	−0.055
HV 1328	1.199645	52.2	2.1	18.59	0.09	−4.47	−5.15	−5.60	−6.00	−6.20	−6.28	0.000	0.020
HV 1333	1.212014	76.5	1.4	19.42	0.04	−4.94	−5.69	−6.20	−6.63	−6.84	−6.92	0.070	−0.005
HV 822	1.223810	62.1	2.2	18.96	0.08	−4.54	−5.38	−5.89	−6.33	−6.67	−6.64	0.030	−0.010

Notes. Column headings are the same as in the previous table.

4.4. The LMC period-luminosity relations

In Table 6 the period-luminosity relations we obtain for the LMC in the different photometric bands are given in the form:

$$M = a(\pm\sigma(a))[\log(P) - 1.0] + b(\pm\sigma(b)). \quad (4)$$

The relations have been determined from a linear regression to the absolute magnitudes and log(P) values given in Table 3. In the table the corresponding relations for the Milky Way sample determined in Paper I are given for comparison. These relations are based on Cepheid distances calculated with exactly the same precepts as in this paper, using the same p-factor relation and IRSB calibration so we can perform a direct comparison of the relations. The relations in the K- and V-bands as well as in the $V,(V-I)$ Wesenheit index are shown in Figs. 4–6 with the Milky Way relations overplotted.

The dispersions of the Milky Way and LMC samples around the ridge line PL relations given in Table 6 are very similar for all the bands, and we note that there is not a big difference in the dispersion as a function of photometric band. The J and K-band values are only marginally smaller than those for the optical bands and the W_{VI} index performs only slightly better than the V-band. If however we consider the LMC Cepheids to be at the same distance we can determine apparent PL relations without involving the individual distances from the IRSB method. In this case the dispersion reduces in W_{VI} from 0.24 to 0.15 mag, in V from 0.26 to 0.19 mag and in the K-band the value even decreases from 0.21 to 0.09 mag. Removing only two stars from the W_{VI} relation further reduces that disperion to 0.09 mag illustrating that the uncertainty on these numbers are quite large due to the small sample size. The fact that the dispersion can be reduced so much by adopting a common distance to all the

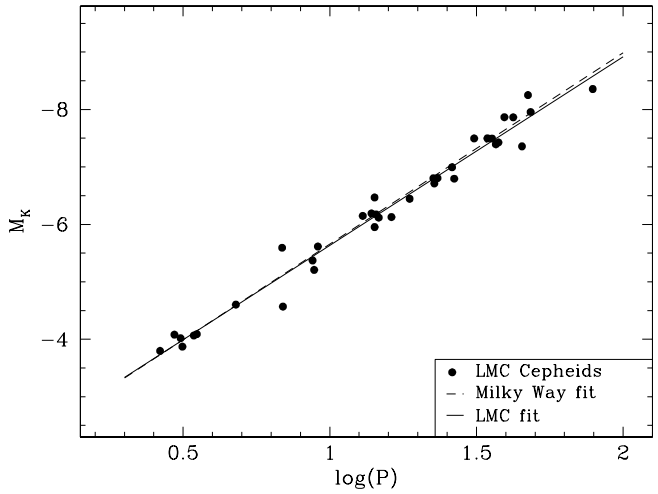

Fig. 4. The K-band period-luminosity relation for our sample of LMC Cepheids based on the absolute magnitudes determined with the IRSB method as calibrated in Paper I. The best fitting line from the data is overplotted in black, and the best fitting line to the Milky Way sample of Paper I is overplotted with a dashed line in red. It is appreciated that the LMC and Milky Way PL relations agree extremely well both in slope and zero point.

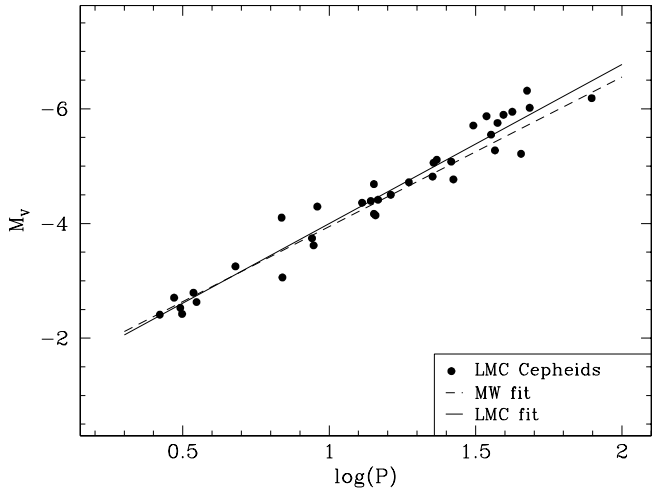

Fig. 5. The V-band PL relation for our sample of LMC Cepheids based on the absolute magnitudes determined by the IRSB method. Overplotted is the linear regression fit (solid line) as well as the corresponding Milky Way relation (dashed line).

stars suggests that the observed dispersion in the PL relations is dominated by errors in the distance moduli rather than intrinsic dispersion in the luminosities or reddening errors and the standard error on the individual distance moduli is about 0.2 mag.

The dispersion of the LMC and MW samples are also very similar suggesting that the LMC data quality is equal to that for the Milky Way sample. Barnes et al. (2005) performed a careful Bayesian analysis of the data presented in Storm et al. (2004) and found that the formal error estimates from the regression fitting, which are also the errors tabulated here in Table 3, were systematically underestimated. On average these errors should be multiplied by a factor of 3.4 to be in agreement with the Bayesian error estimates. In fact the error estimates for the distance moduli presented in Table 3 have a mean value of 0.051 mag, which results in a revised mean error estimate of 0.17 mag, very similar to

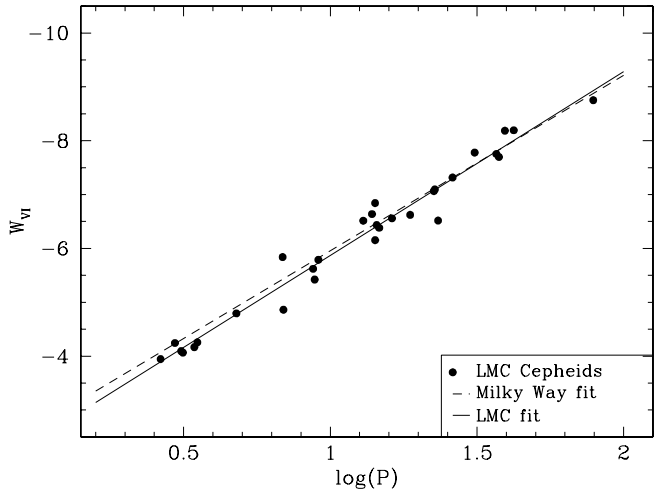

Fig. 6. The optical $(V - I)$ Wesenheit index PL relation for our sample of LMC Cepheids, based on the absolute magnitudes determined by the IRSB method as calibrated in Paper I. Overplotted is the linear regression fit (solid line) as well as the corresponding Milky Way relation (dashed line).

the standard error of 0.2 mag estimated above from the K-band PL relation.

4.5. The effect of metallicity

The LMC Cepheid PL relations in Table 6 can be compared directly to the relations derived in Paper I for the Milky Way sample which have been tabulated for convenience in Table 6. The slopes of the relations are in excellent agreement in the case of the near-infrared J and K bands. In the V band and in the Wesenheit indices, the agreement is slightly worse but well within one σ, whereas the I band slopes differ at the level of about one σ. Since the slopes of the PL relations for both LMC and Milky Way Cepheids are very well constrained from our samples, we conclude that our results present strong evidence that the slope of the Cepheid PL relation, particularly in the near-infrared J and K bands, is identical for the solar metallicity Milky Way and more metal-poor LMC samples. These PL relations are thus independent of metallicity in the range from solar to LMC metallicity. The universality of the PL relation slopes appears to be confirmed in this metallicity range.

We can further extend the metallicity baseline by including the 5 SMC Cepheids in the sample. Given the low number of Cepheids and the narrow range of periods for these stars, we cannot constrain the slope of the PL relation at this metallicty, but we can constrain the zero point offset. In Fig. 7 we have overplotted the SMC Cepheids on the LMC Cepheids for the K-band and obviously there is good agreement. Considering the excellent agreement between the LMC and the Milky Way from Table 6 this further supports the universality of the zero point of the K-band relation.

We can quantify any offsets in the PL relation magnitude zero points as a function of metallicity by comparing the zero point offset for each of the three samples with the reference PL relations determined in Paper I on the basis of all available Cepheids. For each band and sample we computed the mean magnitude offsets, tabulated them in Table 7 and plotted them as a function of metallicity in Fig. 8. For each band we have fit the weighted least square regression line to the magnitude offset as a function of metallicity. The resulting metallicity effect

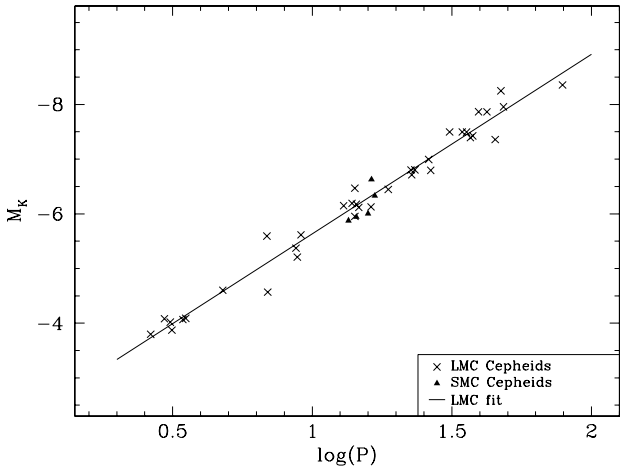

Fig. 7. The K-band absolute magnitudes for our sample of SMC Cepheids (filled triangles) overplotted on the LMC Cepheid PL relation (Fig. 4), crosses are the individual LMC Cepheids.

Table 5. Derived LMC true distance modulus and the slope of the individual Cepheid distance moduli as a function of their pulsation period, for different p-factor relations (see text) $p = \beta_p + \alpha_p \log P$.

α_p	β_p	$(m-M)_0$	$(m-M)_0$ slope
−0.03	1.39	18.50 ± 0.04	0.31 ± 0.10
−0.08	1.31	18.26 ± 0.04	0.22 ± 0.10
−0.08	1.455	18.50 ± 0.04	0.24 ± 0.10
−0.186	1.550	18.45 ± 0.04	0.00 ± 0.10

Table 6. Period-luminosity relations for the LMC in the various optical and near-infrared bands as determined from a linear regression to the absolute magnitudes from the IRSB analysis.

Band	a (mag dex^{-1})	b (mag)	Dispersion (mag)
M_V (LMC)	−2.78 ± 0.11	−4.00 ± 0.05	0.26
M_V (MW)	−2.67 ± 0.10	−3.96 ± 0.03	0.26
M_I (LMC)	−3.02 ± 0.10	−4.74 ± 0.04	0.21
M_I (MW)	−2.81 ± 0.10	−4.76 ± 0.03	0.23
W_{VI} (LMC)	−3.41 ± 0.11	−5.87 ± 0.05	0.24
W_{VI} (MW)	−3.26 ± 0.11	−5.96 ± 0.04	0.26
M_J (LMC)	−3.22 ± 0.09	−5.17 ± 0.04	0.21
M_J (MW)	−3.18 ± 0.09	−5.22 ± 0.03	0.22
M_K (LMC)	−3.28 ± 0.09	−5.64 ± 0.04	0.21
M_K (MW)	−3.33 ± 0.09	−5.66 ± 0.03	0.22
W_{JK} (LMC)	−3.31 ± 0.09	−5.95 ± 0.04	0.21
W_{JK} (MW)	−3.44 ± 0.09	−5.96 ± 0.03	0.23

Notes. The relations have been fitted in the form $M = a[\log(P) - 1] + b$. The fourth column gives the dispersion around the fit. Our results for the Milky Way Cepheids are included for comparison.

slopes have been tabulated in Table 7. We estimate the error on the slopes to be of the order 0.10 mag dex^{-1} based on the error bars on the individual points and the fact that the baseline is smaller than one dex. From Fig. 8 and Table 7 it can be seen that a zero metallicity effect *cannot* be ruled out by the data in most cases but that the effect is significant and the strongest for the W_{VI} index. For extra-galactic distance determination most Cepheid samples will have metallicities in the range from LMC

Table 7. Offsets of each metallicity sample (Milky Way, LMC, and SMC) with respect to the reference PL relations from Paper I, i.e. assuming a fixed PL relation slope irrespective of metallicity.

Band	Δb(MW) (mag)	Δb(LMC) (mag)	Δb(SMC) (mag)	γ (mag dex^{-1})
M_V	+0.02	−0.03	−0.00	+0.09
M_I	−0.00	+0.01	+0.08	−0.06
W_{VI}	−0.03	+0.04	+0.18	−0.23
M_J	−0.01	+0.03	+0.06	−0.10
M_K	−0.01	+0.02	+0.10	−0.11
W_{JK}	−0.00	+0.01	+0.13	−0.10
σ	±0.03	±0.04	±0.11	±0.10

Notes. The last column gives the slope, γ, of the weighted linear regression fit to the data.

to solar and the zero-point offsets in this range is clearly very small in all the bands.

The only bands for which we have excellent agreement between the PL relation slopes are the J and K bands, and the zero-point offsets in both of these bands are small so they each form an excellent basis for a standard candle. In the V band and the W_{JK} index the PL relation slopes are marginally in agreement and also for these two bands the zero-point offsets are small. The I band and the W_{VI} index have significant differences in the PL slopes. The W_{VI} index zero-point is also significantly more metallicity dependent than is the case for the other bands making this index inferior to the J and K-bands as a standard candle.

We note that we have assumed a simple linear metallicity dependence, but it is of course entirely possible that the dependence, if present, has a more complex functional form.

We emphasize that the metallicity effect on both the slopes and zero points discussed here is *entirely independent of the choice of the p-factor relation*, whereas the absolute values of the slopes and zero points as well as the resulting LMC and SMC distances do depend on the adopted p-factor relation.

5. Discussion

We can now compare the slopes of our LMC PL relations with independent measures from apparant magnitudes versus log(P). In the near-infrared we use the relations from Persson et al. (2004) which is based on 92 LMC Cepheids with excellent J and K light curves. They found slopes of -3.261 ± 0.042 and -3.153 ± 0.051 in K and J respectively, in excellent agreement with our values of -3.28 ± 0.09 and -3.22 ± 0.09. In the optical we can compare to the relations from the OGLE project (Udalski 2000) and we similarly find very good agreement. They find in the V and I-bands slopes of -2.775 ± 0.031 and -2.977 ± 0.021, to be compared with our values of -2.78 ± 0.11 and -3.02 ± 0.10 respectively. The fact that we reproduce the slopes of the PL relations in the LMC so well strongly supports our empirical calibration of the p-factor used with the IRSB method and confirms our earlier results (Gieren et al. 2005a) based on a much smaller sample of LMC Cepheids.

The LMC distance modulus of 18.45 ± 0.04 is only slightly shorter than the "canonical" value of 18.50 ± 0.10 as adopted by Freedman et al. (2001) and by the ARAUCARIA project (Gieren et al. 2005b; Pietrzyński et al. 2010a), and slightly longer than the value of 18.39 ± 0.01(random) ± 0.07(systematic) suggested by Freedman & Madore (2010) in their recent review. It is thus in good agreement with most recent results, as would be expected considering that we (see Paper I) have

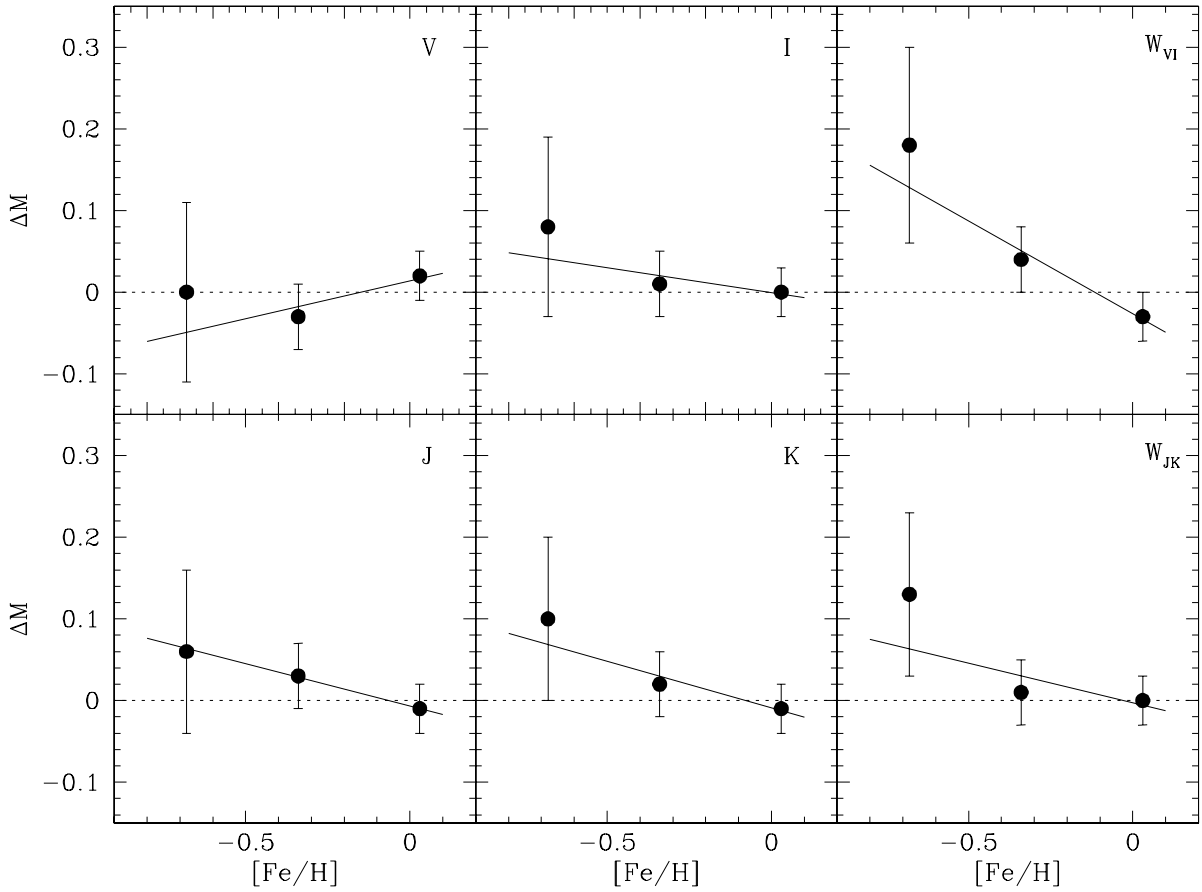

Fig. 8. The zero point offsets, $\Delta M = M - M_{\rm comb}$, for each band with respect to the reference PL relations from Paper I as a function of sample metallicity. The full lines show the weighted linear regression fit to the data. It can be seen that especially in the limited but for extragalactic distance determination most important metallicity range from LMC to solar abundance, the zero point offsets are in general indistinguishable from zero.

calibrated the IRSB method to match the distances to nine Milky Way Cepheids with direct parallaxes from Benedict et al. (2007). These distances are accurate to 4–10%, which seems the largest single remaining systematic uncertainty in the IRSB method assuming that the p-factor relation has been accurately established from our new and improved constraints (which is supported by the arguments given above). The total systematic uncertainty of our present determination of the LMC distance is difficult to quantify, but expected to be about ±5%, which is better than most other techniques which have been used to measure the LMC distance over the years. An exciting possibility to constrain the IRSB method even further, in a very direct way, will be the comparison of the IRSB-determined distance to the LMC Cepheid OGLE-LMC-CEP0227 which is a member in a double-lined eclipsing binary system (Pietrzynski et al. 2010b). Work is underway to determine the distance to this binary from orbital analysis.

In Sect. 4.5 we compared the slopes of the PL relations from the Milky Way and LMC samples finding insignificant differences in the near-IR bands and small (but possibly also non-significant) differences in the optical bands. This result is in good agreement with the findings by Gieren et al. (2005a) but at odds with earlier findings by us (Fouqué et al. 2003; Storm et al. 2004) where we found that the slope of the galactic relations were significantly steeper than those in the LMC and SMC. The reason for this difference was the inappropriate p-factor relation used in the earlier work for determining the Milky Way PL relations. Note that in the present work the choice of the p-factor relation has no bearing on the difference in slope between the Milky Way and LMC PL relations as we are now applying the method to both samples of Cepheids, this was not possible previously as the necessary data for the LMC stars was not yet available. Sandage (2004) also argued that there is a significant difference in slope between the Milky Way and LMC PL relations in the optical bands, the Milky Way relation being steeper. This conclusion was largely based on these older IRSB results, as well as on Cepheids in OB associations from Feast (1999). As we show in Paper I the revised IRSB distances are, apart from a small zero point offset, in very good agreement with the latest results on open cluster Cepheids from Turner (2010) and does not exhibit a period dependence.

We do not support the conclusion of a strong effect of metallicity on the slope of optical (V, I) Cepheid PL relations as reached, for example, by Tammann et al. (2011) or Storm et al. (2004), in fact we find that for these bands the Milky Way PL relations are slightly shallower than the LMC relations, only for the W_{JK} index we find that the Milky Way relation is steeper than the LMC relation.

In Table 7 we summarized the PL relation zero point variation as a function of metallicity. We have made the simplest assumption of a linear relation and found the slopes of the zero point offset versus metallicity relations, γ. Clearly the effects in the near-IR are small and even in the V band the effect appears to be small, albeit with the opposite sign as for the other bands.

The largest effect we find is in the W_{VI} index and our value of $\gamma(W_{VI}) = -0.23 \pm 0.10$ mag dex^{-1} is in excellent agreement with the value of -0.24 ± 0.05 mag dex^{-1}found by Sakai et al. (2004) and other measurements which have been adopted in the recent review paper by Freedman & Madore (2010). This result is slightly at odds with the findings of Bono et al. (2010) who on the basis of data on 48 external galaxies finds no significant metallicity effect on neither slope nor zero point for the Wesenheits indices W_{VI} and W_{JK}. At the same time we do agree with them that the PL relation slopes are less affected in the J and K-bands and more affected in the optical V and I bands and we also agree on the most likely sign of the effect namely that metal-rich PL relations are shallower than metal-poor ones.

It is interesting to note that the most significant metallicity effect is found for the W_{VI} index and that this effect can largely be attributed to the colour difference between Milky Way and LMC Cepheids as found by Sandage et al. (2004). They compared period-colour relations for both Milky Way and LMC Cepheids and found that the LMC Cepheids for a given period are bluer by about 0.05 mag. Feeding this into the Wesenheits index ($W_{VI} = V - 2.54(V - I)$), we find an offset of $0.00 - 2.54 \times -0.05 = 0.13$ mag in the case where the offset is fully in the I-band and $-0.05 - 2.54 \times -0.05 = 0.08$ mag in the case where the effect is fully in the V-band. Disregarding the subtle effects of differences in the slopes of the period-colour relations, these results are comparable to the offset of 0.09 mag, metal-poor Cepheids being fainter, which we find between the Milky Way and LMC W_{VI} relations in Table 6 at a period of 10 days.

The emerging conclusion based on our data and analysis is that for accurate distance measurements to galaxies the K-band Cepheid PL relation is the best suited tool: it is metallicity-independent both regarding the slope and the zero point, it is very insensitive to reddening, and it has a smaller intrinsic dispersion than any optical PL relation. It is likely, as indicated in recent work from Spitzer data, that mid-infrared Cepheid PL relations are even superior to their near-infrared relations because of their even lower sensitivity to reddening, and lower intrinsic dispersions (Madore et al. 2009). Yet, their dependence on metallicity has still to be investigated and they cannot be exploited from the ground making them exceedingly expensive to use.

6. Conclusions and summary

We have obtained new and very accurate radial velocity curves for 22 LMC Cepheids thus expanding the sample of LMC Cepheids to 36 for which we can apply the IRSB distance analysis. We have applied the newly calibrated IRSB technique of Paper I to these 36 LMC Cepheids as well as to 5 SMC Cepheids. The IRSB analysis yields individual distances from which we calculate absolute magnitudes in optical and near-infrared bands. These magnitudes define tight period-luminosity relations in the V, I, J, K bands and in the Wesenheit indices.

We show that the PL relations are in excellent agreement with the observed apparent magnitude versus $\log(P)$ relations in both the optical and near-IR bands lending strong support to the empirical calibration of the p-factor relation in Paper I.

By comparing the LMC Cepheid PL relations to their Milky Way counterparts reported in Paper I that were established with exactly the same precepts, we find practically identical Milky Way and LMC PL relation slopes in the near-infrared bands, arguing for the universality of the Cepheid PL relation in this spectral range. The zero points exhibit a slight metallicity effect, $\gamma(M_K) = -0.10 \pm 0.10$ mag dex^{-1} in the sense that metal-poor Cepheids are fainter than metal-rich Cepheids. If we restrict ourselves only to the metallicity range between solar and LMC, our results are consistent with universal PL relations (in both slope and zero point) in the near-infrared J and K bands.

In the optical bands, we find that the slopes depend weakly on metallicity, the Milky Way slopes being slightly shallower than the LMC slopes, but this difference might not be significant.

The optical PL relation zero points exhibit a metallicity effect of similar size as in the near-IR albeit the sign is opposite in the V-band. The W_{VI} index shows the strongest zero point effect on metallicity where we find $\gamma(W_{VI}) = -0.23 \pm 0.10$ mag dex^{-1}. We stress that the zero-point offsets are based on a rather long metallicity baseline ranging from SMC to solar metallicity.

Our direct distances to the LMC Cepheids leads to a true LMC distance modulus of 18.45 ± 0.04 mag, with an estimated systematic uncertainty of 5% which mainly comes from the uncertainty on the HST parallaxes of nine Milky Way Cepheids that have been used to define the absolute zero point of the IRSB technique. Our distances to the SMC Cepheids leads to an SMC distance of 18.92 ± 0.14.

Both the W_{VI} metallicity effect and the LMC distance which we find are in agreement with the latest values adopted by Freedman & Madore (2010) in their recent review on the Hubble constant.

Considering the significant metallicity effect on the W_{VI} index, not only on the zero-point but most likely also on the slope, we argue that the best standard candle is presently provided by the PL relation in the K-band as it is metallicity insensitive, reddening insensitive and exhibits the lowest intrinsic scatter.

Acknowledgements. We thank Roeland van der Marel for providing his code for computing the LMC distance correction for the stars. A great thanks is due to the La Silla support staff and in particular to the service mode team which managed so well to cover the phase gaps left after the first visitor mode run. We gratefully acknowledge financial support for this work from the Chilean Center for Astrophysics FONDAP 15010003, and from the BASAL Centro de Astrofisica y Tecnologias Afines (CATA) PFB-06/2007.

References

Baranne, A., Queloz, D., Mayor, M., et al. 1996, A&AS, 119, 373
Barnes, T. G. 2009, AIP Conf. Proc., 1170, 3
Barnes, T. G., & Evans, D. S. 1976, MNRAS, 174, 489
Barnes, T. G., Storm, J., Jefferys, W. H., Gieren, W. P., & Fouqué, P. 2005, ApJ, 631, 572
Benedict, G. F., McArthur, B. E., Feast, M. W., et al. 2007, AJ, 133, 1810
Bono, G., Caputo, F., Marconi, M., & Musella, I. 2010, ApJ, 715, 277
Cardelli, J. A., Clayton, G. C., & Mathis, J. S. 1989, ApJ, 345, 245
Carter, B. S. 1990, MNRAS, 242, 1
Cioni, M.-R. L., van der Marel, R. P., Loup, C., & Habing, H. J. 2000, A&A, 359, 601
Feast, M. 1999, PASP, 111, 775
Fouqué, P., & Gieren, W. 1997, A&A, 320, 799
Fouqué, P., Storm, J., & Gieren, W. P. 2003, Lect. Notes Phys., 635, 21
Fouqué, P., Arriagada, P., Storm, J., et al. 2007, A&A, 476, 73
Freedman, W. L., & Madore, B. F. 1990, ApJ, 365, 186
Freedman, W. L., & Madore, B. F. 1991, PASP, 103, 933
Freedman, W. L., & Madore, B. F. 2010, ARA&A, 48, 673
Freedman, W. L., Madore, B. F., Gibson, B. K., et al. 2001, ApJ, 553, 47
Gieren, W., Storm, J., Barnes, T., et al. 2005a, ApJ, 627, 224
Gieren, W., Pietrzyński, G., Soszyński, I., et al. 2005b, ApJ, 628, 695
Groenewegen, M. A. T. 2008, A&A, 488, 25
Hilker, M., Richtler, T., & Gieren, W. 1995, A&A, 294, 648
Hill, V., François, P., Spite, M., Primas, F., & Spite, F. 2000, A&A, 364, 19
Hindsley, R. B., & Bell, R. A. 1989, ApJ, 341, 1004
Imbert, M. 1987, A&A, 175, 30
Kaufer, A., Stahl, O., Tubbesing, S., et al. 1999, The Messenger, 95, 8
Kennicutt, R. C., Jr., Stetson, P. B., Saha, A., et al. 1998, ApJ, 498, 181

Kervella, P., Bersier, D., Mourard, D., et al. 2004, A&A, 428, 587
Kochanek, C. S. 1997, ApJ, 491, 13
Luck, R. E., Moffett, T. J., Barnes, T. G., & Gieren, W. P. 1998, AJ, 115, 605
Madore, B. F., Freedman, W. L., Rigby, J., et al. 2009, ApJ, 695, 988
Mayor, M., Pepe, F., Queloz, D., et al. 2003, The Messenger, 114, 20
Moffett, T. J., Gieren, W., Barnes, T. G., & Gomez, M. 1998, ApJS, 117, 135
Nardetto, N., Mourard, D., Mathias, P., Fokin, A., & Gillet, D. 2007, A&A, 471, 661
Nardetto, N., Gieren, W., Kervella, P., et al. 2009, A&A, 502, 951
Pepe, F., Mayor, M., Galland, F., et al. 2002, A&A, 388, 632
Persson, S. E., Madore, B. F., Krzemiński, W., et al. 2004, AJ, 128, 2239
Pietrzyński, G., Gieren, W., Hamuy, M., et al. 2010a, AJ, 140, 1475
Pietrzyński, G., Thompson, I. B., Gieren, W., et al. 2010b, Nature, 468, 542
Romaniello, M., Primas, F., Mottini, M., et al. 2008, A&A, 488, 731
Sakai, S., Ferrarese, L., Kennicutt, R. C., Jr., & Saha, A. 2004, ApJ, 608, 42
Sandage, A., & Tammann, G. A. 2006, ARA&A, 44, 93
Sandage, A., Tammann, G. A., & Reindl, B. 2004, A&A, 424, 43
Sandage, A., Tammann, G. A., & Reindl, B. 2009, A&A, 493, 471
Sasselov, D. D., Beaulieu, J. P., Renault, C., et al. 1997, A&A, 324, 471
Soszyński, I., Poleski, R., Udalski, A., et al. 2008, Acta Astron., 58, 163
Storm, J., Carney, B. W., Gieren, W. P., et al. 2004, A&A, 415, 531
Storm, J., Gieren, W. P., Fouqué, P., Barnes, T. G., & Gómez, M. 2005, A&A, 440, 487
Storm, J., W. Gieren, & P. Fouqué, et al. 2011, A&A, 534, A94 (Paper I)
Tammann, G. A., Reindl, B., & Sandage, A 2011, A&A, 531, A134
Turner, D. G. 2010, Astrophys. Space Sci., 326, 219
Udalski, A. 2000, Acta Astron., 50, 279
Udalski, A., Wyrzykowski, L., Pietrzyński, G., et al. 2001, Acta Astron., 51, 221
Udalski, A., Szymański, M. K., Soszyński, I, & Poleski, R. 2008, Acta Astron., 58, 69
van der Marel, R., & Cioni, M.-R. 2001, AJ, 122, 1807